Iron(II) and Hydrogen Peroxide Detoxification by Human H-Chain Ferritin. An EPR Spin-Trapping Study†

Guanghua Zhao,*,‡ Paolo Arosio,§ and N. Dennis Chasteen*,‡

Department of Chemistry, University of New Hampshire, Durham, New Hampshire 03824, and Chemistry Section, Faculty of Science, University of Brescia, 25123 Brescia, Italy

Received November 30, 2005; Revised Manuscript Received January 13, 2006

ABSTRACT: Overexpression of human H-chain ferritin (HuHF) is known to impart a degree of protection to cells against oxidative stress and the associated damage to DNA and other cellular components. However, whether this protective activity resides in the protein's ability to inhibit Fenton chemistry as found for Dps proteins has never been established. Such inhibition does not occur with the related mitochondrial ferritin which displays much of the same iron chemistry as HuHF, including an Fe(II)/H_2O_2 oxidation stoichiometry of ∼2:1. In the present study, the ability of HuHF to attenuate hydroxyl radical production by the Fenton reaction ($Fe^{2+} + H_2O_2 \rightarrow Fe^{3+} + OH^- + \cdot OH$) was examined by electron paramagnetic resonance (EPR) spin-trapping methods. The data demonstrate that the presence of wild-type HuHF during Fe^{2+} oxidation by H_2O_2 greatly decreases the amount of ·OH radical produced from Fenton chemistry whereas the ferroxidase site mutant 222 (H62K + H65G) and human L-chain ferritin (HuLF) lack this activity. HuHF catalyzes the pairwise oxidation of Fe^{2+} by the detoxification reaction [$2Fe^{2+} + H_2O_2 + 2H_2O \rightarrow 2Fe(O)OH_{core} + 4H^+$] that occurs at the ferroxidase site of the protein, thereby preventing the production of hydroxyl radical. The small amount of ·OH radical that is produced in the presence of ferritin (≤1% of the iron oxidized) appears to arise from the reaction of H_2O_2 with Fe(III) in the protein rather than from simple Fenton chemistry. The results are discussed in terms of recent experiments reporting both protective and degradative effects of ferritin iron on the integrity of nuclear DNA.

Iron is an essential element (*1*, *2*). Its ability to form complexes such as heme and iron−sulfur clusters in proteins as well as diiron enzymes endows the cell with a variety of functions (*1*−*3*). However, free iron is toxic because it facilitates the generation of highly reactive oxy radical species that can damage cellular constituents. Balancing the deleterious and beneficial effects of iron is an essential aspect of cell survival.

Ferritin plays a central role in the cellular metabolism of iron for almost all organisms. Mammalian ferritins are commonly heteropolymers of 24 subunits of H and L types (∼21000 and ∼19500 Da, respectively) with 55% amino acid sequence identity. The subunits assemble into nearly spherical molecules of 125 Å outer diameter with a hollow interior of about 80 Å (*1*, *2*). Functionally, the H-chain contains a dinuclear ferroxidase center of A and B binding sites consisting of coordinating residues His65 and Glu27 for site A and Glu61, Glu107, and Tyr34 for site B; the two sites are bridged by Glu62 through a coordination bond and by Gln141 through a hydrogen bond. This center facilitates the rapid oxidation of Fe(II) by O_2 or H_2O_2 followed by Fe(III) hydrolysis and mineralization to form the iron core within the protein interior (*4*). In contrast to the H-chain, the more acidic L-subunit lacks a ferroxidase center. However, the L-chain contains a putative nucleation site consisting of a cluster of negative Glu53, Glu56, and Glu57, which appears to be important for slower iron oxidation and mineralization (*5*).

The incorporation of iron into H-chain- or similar subunit-containing ferritins has been studied extensively in vitro (*1*, *2*, *4*−*18*). At low flux of Fe(II) into ferritin (≤2Fe(II)/H-chain), Fe(II) oxidation by O_2 is processed completely by the ferroxidase site with an Fe(II)/O_2 stoichiometry of 2:1, resulting in the quantitative production of H_2O_2 as in eq 1

$$2Fe^{2+} + O_2 + 4H_2O \rightarrow 2Fe(O)OH_{(core)} + H_2O_2 + 4H^+ \quad (1)$$

(*10*−*13*). In human H-chain ferritin (HuHF),[1] Fe(II) oxidation by O_2 produces a μ-1,2-peroxo diferric intermediate at the ferroxidase site that decays to a related intermediate and then to a μ-oxo diferric complex(es) and ultimately to the mineral

† This work was supported by Grant R01 GM20194 from the National Institute of General Medical Sciences (to N.D.C.) and Grant MIUR-FIRB (to P.A.).

* To whom correspondence should be addressed. G.Z.: College of Food and Nutritional Engineering, China Agricultural University (East Campus), Beijing 100083, PR China; phone, +86-10-62737464; fax, +86-10-62737434; e-mail, gzhao318@yahoo.com.cn. N.D.C.: phone, (603) 862-2520; fax, (603) 862-4278; e-mail, dennis.chasteen@unh.edu.

‡ University of New Hampshire.

§ University of Brescia.

[1] Abbreviations: BSA, bovine serum albumin; DMPO, 5,5-diethyl-1-pyrroline *N*-oxide; EcBFR, *Escherichia coli* bacterioferritin; EPR, electron paramagnetic resonance; HoSF, horse spleen ferritin; HuHF, human H-subunit ferritin; HuLF, human L-subunit ferritin; EMPO, 5-ethoxycarbonyl-5-methyl-1-pyrroline *N*-oxide; DEPMPO, 5-diethoxyphosphoryl-5-methyl-1-pyrroline *N*-oxide; Mes, 2-(*N*-morpholino)-ethanesulfonic acid; Mops, 3-(*N*-morpholino)propanesulfonic acid; mutant 222, E62K + H65G variant of HuHF; PBN, phenyl *N*-*tert*-butylnitrone; TEMPO, 2,2,6,6-tetramethylpiperidine-*N*-oxyl.

10.1021/bi052443r CCC: $33.50
Published on Web 02/17/2006

core (*6*, *7*, *14*, *15*). Beyond 48 Fe(II)/HuHF [2 Fe(II)/ferroxidase site] added, some of the H_2O_2 produced at the ferroxidase site rapidly reacts with further Fe(II) via the detoxification reaction given by eq 2 (*4*) and possibly with other components in the reaction mixture (*11*, *17*, *18*).

$$2Fe^{2+} + H_2O_2 + 2H_2O \rightarrow 2Fe(O)OH_{(core)} + 4H^+ \quad (2)$$

At 48 Fe(II)/protein, reactions 1 and 2 have very similar rates in HuHF when the same concentrations of the two oxidants are employed (*18*), a situation unlike that of *Escherichia coli* bacterioferritin where reaction 2 is much faster than reaction 1 (*16*). Thus, the observed Fe(II)/O_2 oxidation stoichiometry of ~2:1 for HuHF (*4*) compared to ~4:1 for EcBFR (*16*) is accounted for by the fact that the small amount of H_2O_2 produced in reaction 1 in HuHF cannot compete with the larger amount of dissolved O_2 in solution for oxidation of Fe(II). Consequently, reaction 2 does not occur to any significant extent in HuHF at a ratio of 48 Fe(II)/protein whereas in EcBFR virtually all of the H_2O_2 produced in reaction 1 is consumed in reaction 2.

There is a growing body of evidence indicating that ferritins play an important role in protecting cells from oxidative stress. Overexpression of HuHF in HeLa and erythroid cells renders the cells resistive to the toxicity of H_2O_2 added to cultures (*19*, *20*). HuHF binds to nuclear DNA of human astrocytoma tumor cells and in short-term assays protects the DNA from oxidative cleavage (*21*). Longer term in vitro assays under a variety of conditions indicate that HuHF may promote damage to DNA due to the mobilization of iron from the protein (*22*). Previous studies have shown that a limited amount of ·OH radical is produced during the oxidative deposition of iron in HuHF and HoSF using DMPO and PBN as spin traps (*23*, *24*).

In the present study, hydroxyl radical spin-trapping experiments were undertaken to better understand the chemistry of HuHF detoxification of activated oxygen species. Here, we show that HuHF greatly attenuates the production of hydroxyl radical from the Fenton reaction when H_2O_2 is the oxidant for Fe(II), consistent with the 2:1 Fe(II)/H_2O_2 oxidation stoichiometry for the detoxification reaction 2 (*4*). However, a 2:1 oxidation stoichiometry by itself does not ensure that Fenton chemistry will not occur (see Discussion). It is demonstrated that functional H-chain ferroxidase sites are required for this activity. A small amount of hydroxyl radical is detected in our experiments using EMPO and DEPMPO spin traps when either H_2O_2 or O_2 is employed as the oxidant. The observed ·OH radical appears to come from the reaction of H_2O_2 with either the μ-oxo diFe(III) complex at the ferroxidase site or the newly formed Fe(III) core.

MATERIALS AND METHODS

All chemicals were of reagent grade or purer. Ferrous sulfate was obtained from Baker Scientific Inc. (Phillipsburg, NJ). Mops and Mes buffers were from Research Organics (Cleveland, OH). EMPO and DEPMPO were purchased from Oxis Research (Portland, OR). Superoxide dismutase (SOD) from bovine erythrocytes (EC 1.15.1.1) of specific activity 3730 units/mg of solid was purchased from Sigma-Aldrich (St. Louis, MO) and beef liver catalase (EC 1.11.1.6) of 6500 units/mg activity from Boehringer-Mannheim GmbH (Germany). 1,10-Phenanthroline was purchased from Aldrich (Milwaukee, WI). Recombinant human H-chain and L-chain ferritins (HuHF and HuLF) and mutant 222 (E62K + H65G) were prepared as previously described (*25*, *26*). The HuHF concentration was determined by the absorbance at 280 nm (ϵ = 23000 M^{-1} cm^{-1} per subunit) (*11*). The mutant 222 and HuLF concentrations were determined by advanced protein assay (http://cytoskeleton.com) using BSA as a standard. The protein was rendered iron free by continuous flow anaerobic dialysis using sodium dithionite and 2,2′-bipyridyl (*27*, *28*).

EPR spectra for Figures 1, 4, 5, and 6 were recorded on a laboratory-assembled EPR spectrometer based on a Bruker ER 041 XK-H X-band microwave bridge operating at 9.24 GHz with 100 kHz field modulation. Samples in 1 mm i.d. quartz capillaries were placed in a Varian TE_{102} cavity for measurement at room temperature. Unless otherwise stated, all spectrometer parameters were as follows: microwave power, 5.0 mW; modulation amplitude, 0.8 G; time constant, 0.3 or 1 s; scan time, 500 s. In the EMPO spin-trapping experiments for hydroxyl radical, all spectra were recorded approximately 1 min after addition of the last reagent. The concentrations of reactants are indicated in the figure captions. The freshly prepared $Fe(O)OH_s$ used in the spin-trapping experiments in the absence of the protein was synthesized by the addition of 400 μM $FeCl_3$ in H_2O (pH ~2) to 25 mM EMPO in 0.1 M Mops buffer, pH 7.0, or to water at pH 7 controlled by a pH stat apparatus described elsewhere (*15*). To determine whether hydroxyl radical is produced from the reaction between Fe(III) and H_2O_2, 1000 μM H_2O_2 was added with stirring to the $Fe(O)OH_s$ suspension in 0.1 M Mops buffer, pH 7.0, or in water at pH 7. The concentration of the hydroxyl radical spin-trap adduct, EMPO−OH, in all experiments was determined by comparison of the double integral of its EPR spectrum with that of a standard solution of 1.0 mM TEMPO in the same buffer.

To determine whether HuHF attenuates the production of hydroxyl radical from the Fenton reaction, 48 μM Fe(II) were added anaerobically to 2.0 μM apoHuHF, apo-mutant 222 of HuHF, apoHuLF, or bovine serum albumin (BSA) plus 25 mM EMPO or DEPMPO in 0.1 M Mops pH 7.0, which had been deoxygenated for 8 h by moist argon, followed by the addition of 150 μM H_2O_2. After 1 min, X-band EPR spectra were recorded on a Bruker EleXsys E500 spectrometer fitted with a high-sensitivity SHQ cavity (Figures 2, 3, and 7). A 2.0 mm i.d. quartz tube holding a 1.0 mm i.d. capillary containing ~40 μL of sample solution was employed. The instrumental conditions were as follows: microwave power, 5.14 mW (16 dB attenuation); microwave frequency, 9.86 GHz; modulation frequency, 100 kHz; modulation amplitude, 0.5 G; receiver gain, 70 dB; time constant, 163.84 ms; sweep time, 83.89 s; sweep width, 70 G for EMPO and 120 G for DEPMPO; center field, 3507 G.

RESULTS

Detection of Hydroxyl Radical during Fe(II) Oxidation by O_2 in HuHF. To examine the production of ·OH radical during the oxidative deposition of iron in ferritin using O_2 as the oxidant, various amounts of iron [50−1000 Fe(II)/HuHF] were added to a 100% O_2-saturated solution of 1.0 μM apoHuHF with 25−35 mM of the spin-trapping reagent EMPO. An EPR signal of the EMPO−OH adduct was

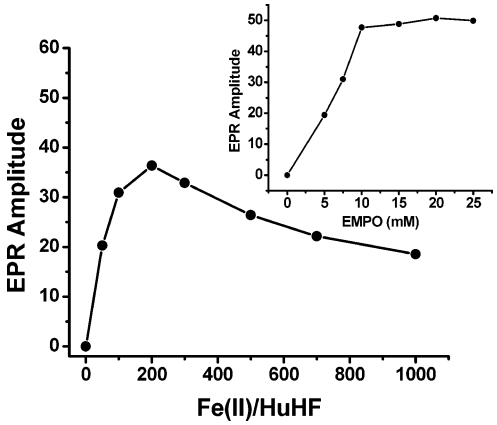

FIGURE 1: EPR signal amplitude of EMPO−OH as a function of Fe(II)/apoHuHF ratio upon Fe(II) oxidation by O_2. Each point represents a separate sample. Conditions: 1.0 μM apoHuHF, 35 mM EMPO, 50−1000 μM $FeSO_4$, 100 mM Mops, pH 7.0, 25 °C, 100% O_2 atmosphere. Inset: EPR signal intensity versus EMPO concentration. Conditions: 1.6 μM apoHuHF, 5−25 mM EMPO, 320 μM $FeSO_4$, in 100 mM Mops, pH 7.0, room temperature, 100% O_2.

observed. A plot of the signal amplitude of the adduct versus the Fe(II)/HuHF ratio is shown in Figure 1. The EPR signal reaches a maximum at 200 Fe(II)/HuHF and then decreases with further Fe(II) loading of the protein. At 200 Fe(II) added, the EPR signal corresponds to a trapped hydroxyl radical concentration of 1.7 μM, or only ~1% of the *total* Fe(II) oxidized, decreasing to ~0.09% at 1000 Fe(II) added when accounting for the 5-fold increase in Fe(II) present, a result indicating minimal ·OH radical production in the protein.

The inset in Figure 1 shows a plot of EPR amplitude of the EMPO−OH adduct versus the concentration of EMPO used when 200 Fe(II)/protein were added to 1.6 μM apoHuHF. The curve levels off above 10 mM EMPO, indicating that the 25−50 mM concentration of EMPO used in the experiments reported here is adequate for the efficient trapping of hydroxyl radical, out-competing other reactions. This result was confirmed by experiments showing that 50 mM buffer does not effectively compete with 25 mM spin trap for reaction with ·OH radical. The same strength EPR signal of the EMPO−OH adduct was obtained for the addition sequence 48 μM $FeSO_4$ + 25 mM EMPO + 150 μM H_2O_2 when the pH 7 of the solution was controlled by either 50 mM Mops or the pH stat apparatus (data not shown). In any case, good pH control is important for quantitative results. The amount of EMPO−OH adduct formed depends strongly on pH, increasing markedly as the pH is lowered (Figure 2). The spectra at pH 7 and 8 are 33% and 15% as intense, respectively, compared to the pH 6 spectrum.

Attenuation of Hydroxyl Radical Production during Fe(II) Oxidation by H_2O_2 in HuHF. The ability of HuHF to attenuate hydroxyl radical production during direct oxidation of Fe(II) by H_2O_2 was examined by spin-trapping experiments employing the reagents EMPO and DEPMPO (*16*, *29*, *30*). All solutions were thoroughly deoxygenated with argon before each experiment. Since HuHF binds only 24 Fe(II)/protein under anaerobic conditions (*31*), this amount of Fe(II) was added anaerobically to the solution of apoHuHF containing the spin-trapping reagent followed by H_2O_2. The

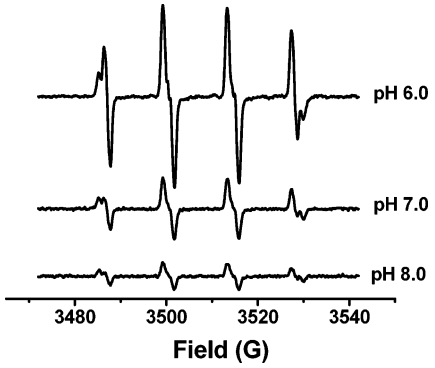

FIGURE 2: Dependence of the EMPO−OH EPR spectrum on pH. Hydroxyl radical was generated by the Fenton reaction. Conditions: 48 μM $FeSO_4$, 25 mM EMPO, 150 μM H_2O_2 in 50 mM MES, pH 6.0, or 50 mM Mops, pH 7.0 or 8.0.

results are shown in Figure 3. Spectrum a in Figure 3A is that of the EMPO−OH adduct for the control experiment in the absence of protein and corresponding to the addition sequence EMPO + Fe(II) + H_2O_2 in Mops, pH 7.0. As expected, a strong EPR signal was observed, indicating the efficient one-electron oxidation of Fe(II) by H_2O_2 through Fenton chemistry. Spectrum b in Figure 3A is another control experiment in the presence of bovine serum albumin with the addition sequence BSA + EMPO + Fe(II) + H_2O_2. Again, an intense EPR signal was seen, indicating that BSA does not appreciably affect the amount of EMPO−OH adduct formed in accord with previous observation (*30*). In contrast, only a weak EPR signal was observed in the presence of ferritin for the addition sequence apoHuHF + EMPO + Fe(II) + H_2O_2 (spectrum e), a result indicating that apoHuHF minimizes the one-electron oxidation reaction of Fenton chemistry. This finding is consistent with the 2 Fe(II)/H_2O_2 oxidation stoichiometry of eq 2 for HuHF reported recently (*4*). When apoHuHF was replaced by either the HuHF ferroxidase site mutant 222 (E62K + H65G) or HuLF, a strong EPR signal was observed (curves c and d, respectively), demonstrating that an intact ferroxidase site is required for detoxification of Fe(II) and H_2O_2. Similar results were obtained with DEPMPO (Figure 3B), demonstrating that the findings are independent of the choice of spin trap.

Production of ·OH from the Reaction of H_2O_2 with the μ-Oxo Diferric Complex. Previous studies have demonstrated that ·OH can be produced from the reaction of H_2O_2 with Fe(III) complexes (*33*−*36*) so the possibility that this chemistry also occurs in HuHF was explored. The reaction of H_2O_2 with the μ-oxo diferric complex of the ferroxidase site was first examined. A series of 12−96 Fe(II)/protein was added aerobically to 4.0 μM apoHuHF in 0.1 M Mops, pH 7.0, and allowed to oxidize for 2 min followed by the addition of 25 mM EMPO and 800 μM H_2O_2. For the ≤48 Fe(II)/HuHF sample, 2 min is sufficient time for the complete formation of the μ-oxo diferric complex but not too long that it clears from the ferroxidase site (*15*). The hydroxyl radical adduct of EMPO was detected. A plot of the EPR amplitude of the EMPO−OH adduct as a function of the Fe(III)/apoHuHF ratio is shown in Figure 4. As the ratio of Fe(III) to apoHuHF increases, the EPR amplitude also increases, reaching a maximum at ~48 Fe(III)/protein addition, suggesting that ·OH is produced from the reaction of H_2O_2 with iron at the 24 ferroxidase sites of the protein.

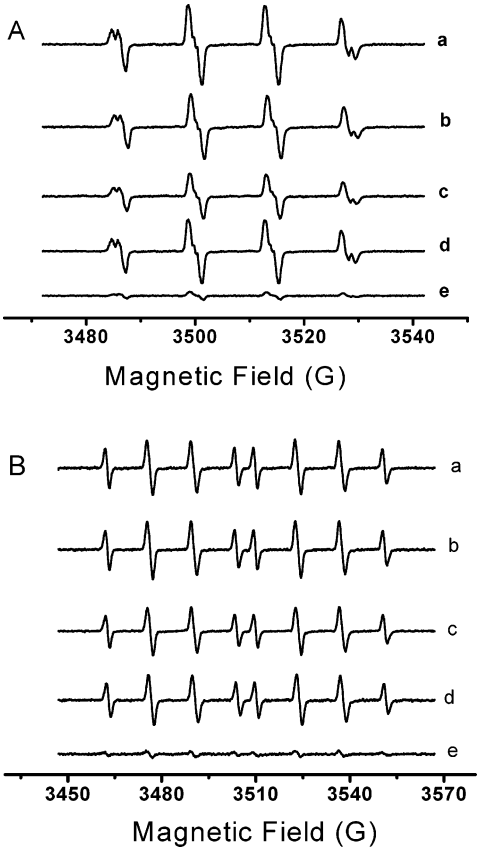

FIGURE 3: X-band EPR signal of the EMPO−OH adduct in the presence and absence of HuHF or HuLF. Panel A: spectrum a, anaerobic addition sequence EMPO + Fe(II) + H_2O_2; spectrum b, anaerobic addition sequence BSA + EMPO + Fe(II) + H_2O_2; spectrum c, anaerobic addition sequence apo-mutant 222 + EMPO + Fe(II) + H_2O_2; spectrum d, anaerobic addition sequence apoHuLF + EMPO + Fe(II) + H_2O_2; spectrum e, anaerobic addition sequence apoHuHF + EMPO + Fe(II) + H_2O_2. Conditions: 2.0 μM apoHuHF or BSA or apo-mutant 222 (E62K + H65G) or apoHuLF, 25 mM EMPO, 48 μM $FeSO_4$, 150 μM H_2O_2, 20 mM Mops, pH 7.0, room temperature. Panel B:, spectrum a, anaerobic addition sequence DEPMPO + Fe(II) + H_2O_2; spectrum b, anaerobic addition sequence BSA + DEPMPO + Fe(II) + H_2O_2; spectrum c, anaerobic addition sequence apo-mutant 222 + DEPMPO + Fe(II) + H_2O_2; spectrum d, anaerobic addition sequence apoHuLF + DEPMPO + Fe(II) + H_2O_2; spectrum e, anaerobic addition sequence apoHuHF + DEPMPO + Fe(II) + H_2O_2. Conditions: 2.0 μM apoHuHF or BSA or apo-mutant 222 or apoHuLF, 25 mM DEPMPO, 48 μM $FeSO_4$, 150 μM H_2O_2, 20 mM Mops, pH 7.0, room temperature.

At 48 Fe/HuHF, the maximum EPR signal corresponds to only ~0.5% of the added iron. At higher Fe(II) loading of the protein, the EPR amplitude decreases presumably because at 2 min no Fe(III) remains at the ferroxidase site and is virtually all present in the core, as previously demonstrated by kinetic studies (*14*). This result suggests that H_2O_2 has a stronger reactivity with the μ-oxo diferric complex than with the Fe(III) core which is more thermodynamically stable.

Production of ·OH from the Reaction of the "Young" Fe(III) Core with H_2O_2. To determine whether ·OH is also formed from the reaction of H_2O_2 with the Fe(III) core, 1000 μM H_2O_2 was added directly to 1.6 μM holoHuHF samples freshly prepared from Fe(II) and apoHuHF by air oxidation overnight and containing an Fe(III)/protein ratio ranging from 50 to 1000. Significantly, an EPR signal from EMPO−OH was again observed. The EPR signal of the adduct as a function of the iron content of the protein is shown in Figure 5 where a maximum is again observed at 200 Fe(III)/HuHF as in Figure 1. This unexpected result prompted us to examine the reactivity of H_2O_2 with hydrous ferric oxide in the absence of protein. In this experiment H_2O_2 was added to a fine precipitate of freshly prepared $Fe(O)OH_{(s)}$ (see Materials and Methods). An EPR signal from the EMPO−OH adduct was once more obtained (Figure 6, spectrum e). However, hydroxyl radical was not detected with EMPO upon the addition of H_2O_2 to holoferritins containing cores of 250−350 Fe(III) which were over 1 month old (data not shown).

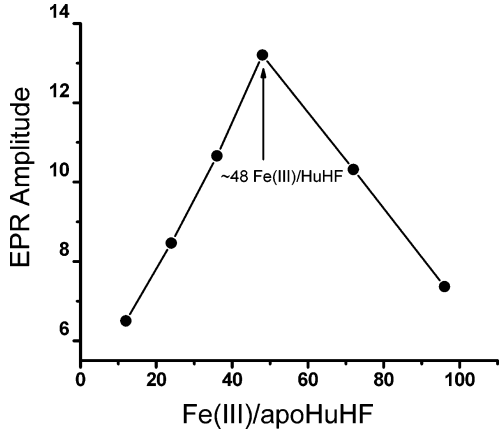

FIGURE 4: EPR signal amplitude of EMPO−OH as a function of the Fe(III)/apoHuHF ratio. Each point represents a separate sample where the Fe(II) was first oxidized aerobically followed by the addition of H_2O_2 2 min later. Conditions: 4.0 μM apoHuHF, 25 mM EMPO, 48−384 μM $FeSO_4$, 800 μM H_2O_2, 0.1 M Mops, pH 7.0, room temperature.

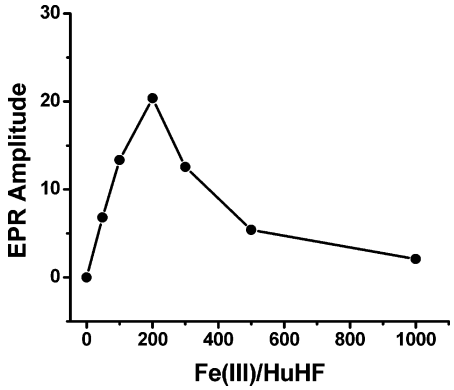

FIGURE 5: EPR signal amplitude of EMPO−OH as a function of the Fe(III)/apoHuHF ratio for freshly prepared cores. Each point represents a separate sample. Conditions: 1.6 μM apoHuHF, 80−1600 μM $FeSO_4$, 25 mM EMPO, 1000 μM H_2O_2, 0.1 M Mops, pH 7.0, room temperature.

Figure 7 shows the effect of catalase and superoxide dismutase on hydroxyl radical formation upon addition of H_2O_2 to freshly prepared ferritin containing 200 Fe(III)/HuHF. Spectrum a is the result of the control experiment in the absence of either enzyme for the addition sequence ferritin + EMPO + H_2O_2. No attenuation of the EPR signal was observed when SOD is included in the reaction mixture with the addition sequence ferritin + EMPO + SOD + H_2O_2 (curve b), suggesting either that superoxide is not produced [and hence not present to reduce the Fe(III) of the core] or that the SOD does not gain access to $O_2^{\cdot -}$ generated inside the protein cavity. The latter interpretation is the more likely

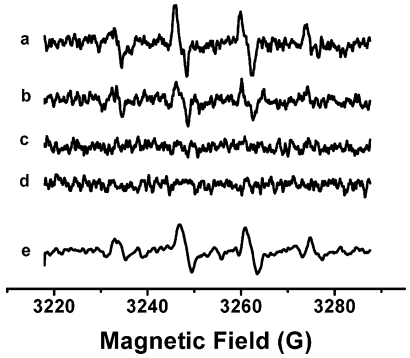

FIGURE 6: X-band EPR signal as an EMPO adduct in the presence of HuLF plus a different amount of Fe(II): (a) apoHuLF + 50 Fe(II)/HuHF; (b) apoHuLF + 100 Fe(II)/HuHF; (c) apoHuLF + 350 Fe(II)/HuHF; (d) apoHuLF + 500 Fe(II)/HuHF. Conditions: 2.7 μM apoHuLF, 25 mM EMPO, 135−1350 μM $FeSO_4$, in 100 mM Mops, pH 7.0, room temperature. (e) $FeCl_3$ + EMPO + H_2O_2. Conditions: 400 μM $FeSO_4$, 25 mM EMPO, 1000 μM H_2O_2, in 100 mM Mops, pH 7.0 or pH 7.0 controlled by pH stat, 25 °C.

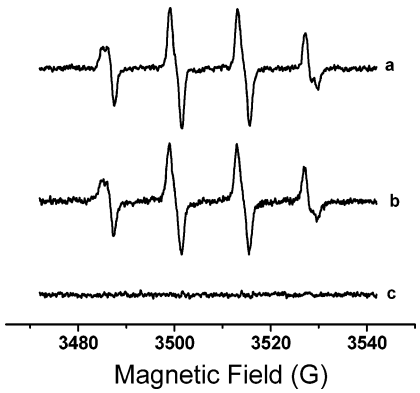

FIGURE 7: X-band EPR spectra of the EMPO−OH adduct formed from the reaction of the iron core of HuHF with H_2O_2 in the absence and presence of SOD and catalase. Spectrum: (a) 200 Fe(III)/protein core + EMPO + H_2O_2; (b) 200 Fe(III)/protein core + EMPO + SOD + H_2O_2; (c) 200 Fe(III)/protein core + EMPO + catalase + H_2O_2. Conditions: 2.0 μM apoHuHF, 200 Fe(III)/protein [which were prepared by adding 200 Fe(II) aerobically to apoHuHF followed by standing overnight], 25 mM EMPO, 120 units mL^{-1} superoxide dismutase, 325 units mL^{-1} catalase, 1000 μM H_2O_2, 50 mM Mops, pH 7.0, room temperature.

one since the presence of SOD consistently caused a 25% reduction in the amount of EMPO−OH formed when H_2O_2 was added to freshly precipitated $Fe(O)OH_{(s)}$ in 50 mM MES, pH 6.5, employing the addition sequence 400 μM or 1 mM Fe(III) + 25 mM EMPO + 125 or 312 units/mL SOD + 1 mM H_2O_2 (data not shown). As anticipated, no EMPO−OH spin-trap adduct was observed when catalase, which disproportionates H_2O_2, was present for the addition sequence ferritin + EMPO + catalase + H_2O_2 (Figure 7, curve c).

Experiments were also conducted to look for measurable reduction of Fe(III) by H_2O_2. A sample of 20 μM HuHF freshly loaded with 800 ^{57}Fe(III)/HuHF was treated anaerobically with 16.4 mM H_2O_2 for 1.5 min and then frozen for Mössbauer measurement. The Mössbauer spectrum showed only spectral lines from the Fe(III) core and no features from Fe(II). The colorimetric ferrous ion chelator 1,10-phenanthroline was then used to detect the formation of Fe(II). A slow rate of Fe(III) reduction over a period of 30 min, corresponding to ~1% of the iron, was observed when 3 mM 1,10-phenanthroline is added anaerobically to 2 μM HuHF [500 Fe(III)/HuHF] in 0.1 M Mops, pH 7, in the absence of H_2O_2. In the presence of 1 mM H_2O_2, the rate was retarded by 8%, not enhanced. Since in this experiment the protein itself is the likely source of reducing equivalents, e.g., cysteine residues, and since 1,10-phenanthroline is a preferential Fe(II) chelator that will favor Fe(III) reduction, an anaerobic experiment was carried out using freshly precipitated $Fe(O)OH_s$ without protein. In this instance, no Fe(II) reduction was observed in either the presence or absence of H_2O_2. Thus none of the above experiments provided evidence for significant Fe(III) reduction by H_2O_2, a result consistent with the low levels of ·OH radical observed.

Detection of Hydroxyl Radical during Fe(II) Oxidation in Human L-Chain Ferritin. Since H_2O_2 is also formed during Fe(II) oxidation and deposition in HuLF (*4*), a series of spin-trapping experiments were carried out to look for the production of ·OH in this protein. Different amounts of Fe(II) were added to 2.7 μM apoHuLF containing EMPO in 0.1 M Mops, pH 7.0. The results are shown in Figure 6 (spectra a−d). The EMPO−OH adduct was formed upon addition of 50 Fe(II)/HuLF (spectrum a), corresponding to only ~0.13% of the Fe(II) oxidized but declining to ~0.04% at 100 Fe(II)/HuLF (spectrum b). No EMPO−OH adduct was observed at 350 or 500 Fe(II)/HuLF (spectra c and d). Thus the production of ·OH depends markedly on the Fe(II)/protein ratio, decreasing with formation of larger cores as the Fe(II)/O_2 stoichiometry approaches 4:1 (*4*).

DISCUSSION

The present work shows that H-chain ferritin greatly attenuates ·OH radical generation from the Fenton reaction and that the ferroxidase site is responsible for this activity (Figure 3). Such a finding could not be predicted a priori on the basis of an observed Fe(II)/H_2O_2 oxidation stoichiometry of 2:1 alone (*4*). An ~2:1 Fe(II)/H_2O_2 stoichiometry has also been observed with mitochondrial ferritin (*37*) and egg albumin (*38*), but neither of these proteins is capable of affecting the amount of ·OH radical generated relative to controls. This is presumably because two one-electron Fe(II) oxidation steps are involved in these proteins (*37*, *38*) whereas a concerted (or nearly so) two-electron oxidation seems to occur in HuHF. Since mitochondrial ferritin and HuHF have similar ferroxidase sites, the reason for this difference is unclear. These findings emphasize the importance of carrying out quantitative spin-trapping experiments to measure hydroxyl radical produced via Fenton chemistry in order to establish whether a particular protein affords protection against oxidative stress.

The marked attenuation of ·OH radical production in the presence of HuHF shown in Figure 3 (curves e) is in accord with in vivo assays of H_2O_2 toxicity (*19*, *20*) and DNA damage (*21*) whereby the wild-type HuHF clones of HeLa, astrocytoma tumor, and erythroid cells are resistive to H_2O_2-induced stress whereas the ferroxidase site mutant 222 and HuLF clones are not. Thus the in vitro measurements of hydroxyl radical production reported here correlate very well with the results of in vivo studies and indicate that the presence of a functional H-chain ferroxidase site is required for detoxification of Fe(II) and H_2O_2. In this respect, HuHF exhibits properties similar to those of bacterial Dps proteins

that protect DNA from oxidative damage (*29*, *30*, *32*) and of bacterioferritin EcBFR (*16*). Presumably, the dinuclear ferroxidase sites of all of these proteins facilitate the pairwise oxidation of Fe^{2+} by H_2O_2, thus avoiding the odd electron oxidation associated with Fenton chemistry.

The concentration of ·OH produced in HuHF from the reaction of H_2O_2 with the Fe(III) core reaches a maximum at 200 Fe(II)/HuHF addition (Figure 5), corresponding to only ~1% of the total Fe(II) oxidized and much less at other iron loadings of the protein. Similar results are seen with O_2 as the oxidant (Figure 1). A plot of Fe(II)/O_2 oxidation stoichiometry versus Fe(II)/HuHF has been previously shown to have a discontinuity at ~200 Fe added and Fe(II)/O_2 stoichiometries of 2.5−2.8, consistent with the presence of some partially reduced oxygen species as observed here. Thus an ~200 Fe/HuHF stoichiometry is observed in a variety of experiments. It appears to be related to the minimum core size for the mineral surface reaction to occur where O_2 is reduced completely to H_2O (*4*).

The production of the small amount of hydroxyl radical during Fe(II) oxidation by O_2 or H_2O_2 shown in Figures 1, 4, and 5 could be due to a small fraction of the iron not oxidized at the ferroxidase site that undergoes the Fenton reaction. However, examination of the data suggests another possibility. Recent studies have shown that the ferroxidase sites of HuHF catalyze reaction 1 at all stages of iron loading of the protein (*4*, *14*). Although the percentage of iron oxidized by this reaction decreases with increasing increments of Fe(II) added to the protein, the *total* amount of H_2O_2 produced by reaction 1 increases (*4*). Thus a 500 or 700 Fe(II)/HuHF sample would be expected to produce more hydroxyl radical than the 200 Fe(II)/HuHF sample if Fenton chemistry alone were the primary source of hydroxyl radical, contrary to what is observed here (Figure 1).

What then is the source of ·OH radical? Figure 4 shows that ·OH is produced from the reaction of H_2O_2 with the μ-oxo diferric complex of the ferroxidase site. The concentration of hydroxyl radical reaches a maximum at 48 Fe(III)/protein, representing ~0.5% of the total Fe(III) loading of protein. However, the plot in Figure 4 exhibits a profile distinct from the curve for Fe(II) oxidation by O_2 (Figure 1), suggesting that the reaction of H_2O_2 with the μ-oxo complex of the ferroxidase site is not the *primary* pathway for ·OH formation during Fe(II) oxidation by O_2.

In contrast, the curve in Figure 5 where H_2O_2 was added directly to the core containing holoHuHF shows a strikingly similar profile to the curve in Figure 1, a result suggesting that the small amount of hydroxyl radical observed primarily stems from the reaction of H_2O_2 with Fe(III) of the newly formed core. A freshly prepared small core of ~200 Fe(III)/HuHF appears to be optimal for this reaction. Support for this conclusion comes from the spin concentration measurement showing that the maximum amount of ·OH radical trapped corresponds to only ~1% of total Fe(III) of the core, the same as the amount of Fe(II) involved in ·OH formation during Fe(II) oxidative deposition in HuHF with O_2 as the oxidant (Figure 1). A direct reaction between H_2O_2 and the core is further supported by the observation that the EMPO−OH adduct is also produced by the simple addition of H_2O_2 to a freshly prepared suspension of $Fe(O)OH_{(s)}$ in the absence of protein (Figure 6, spectrum e). The lack of ·OH production upon addition of H_2O_2 to aged ferritins (1 month old) containing 250−350 Fe(III)/protein (Results) may be ascribed to increased inertness of their mineral phases, perhaps due to increased size and crystallinity of their cores as they age.

Hydroxyl radical has been previously reported to form from the reaction of H_2O_2 with a variety of Fe(III) complexes (*33*, *35*, *36*, *39*) or with free Fe(III) (*34*). Reaction between $FeCl_3$ and H_2O_2 in the absence of ferritin has been shown to lead to DNA strand breaks (*22*) and is probably caused by the same chemistry observed in the present experiments with ferritin where H_2O_2 reacts with Fe(III) to produce ·OH radical. There are two schools of thought on how formation of ·OH radical might occur from a reaction between Fe(III) and H_2O_2. One proposal is that the iron catalyzes the disproportionation of H_2O_2 to form superoxide ($O_2\cdot^-$) and H_2O and in the process goes through a ferryl (FeO^{2+}) intermediate (*36*). The $O_2\cdot^-$ produced then reduces Fe(III) to Fe(II) which reacts with H_2O_2 by the Fenton reaction. In such instances, SOD inhibits ·OH formation (*36*). SOD has no effect on the EMPO−OH adduct formation in ferritin (Figure 7), possibly because the enzyme is precluded from the interior of the protein shell where the superoxide is generated. However, SOD does have an effect on EMPO−OH formation when H_2O_2 is added to freshly precipitated $Fe(O)OH_s$ so a reduction mechanism involving $O_2\cdot^-$ is a possibility in ferritin. Superoxide is known to reduce Fe(III) of the core of ferritin although the amount of reduction is limited (*40*), a result consistent with the limited amount of ·OH radical seen with HuHF. In ferritin, one possibility is that Fe^{3+} of the core might undergo a series of reactions as follows, where the iron cycles between oxidation states +2, +3, and +4 analogous to the mechanism postulated for the reaction between Fe^{3+}-EDTA and H_2O_2 (*36*):

$$Fe^{3+}_{(core)} + 2H_2O_2 \rightarrow FeO^{2+}_{(core)} + O_2\cdot^- + H_2O + 2H^+$$

$$FeO^{2+}_{(core)} + H_2O_2 \rightarrow Fe^{3+}_{(core)} + O_2\cdot^- + H_2O$$

$$Fe^{3+}_{(core)} + O_2\cdot^- \rightarrow Fe^{2+}_{(aq)} + O_2$$

$$Fe^{2+}_{(aq)} + H_2O_2 \rightarrow Fe^{3+}_{(core)} + OH^- + \cdot OH$$

An alternate proposal is that H_2O_2 directly reduces Fe(III) to produce Fe(II) and $O_2\cdot^-$; the Fe(II) then reacts with H_2O_2 by the Fenton reaction (*34*). However, this mechanism seems to be favored in acidic media where free Fe(III) is present. Both mechanisms ultimately result in production of some Fe(II). However, neither Mössbauer spectroscopy nor 1,10-phenanthroline have provided any direct evidence for Fe(III) reduction by H_2O_2 in ferritin at physiological pH (see Results). If such reduction does occur, it does so at a level that it is undetectable in our experiments, a result that is also consistent with the limited amount of ·OH radical observed with HuHF. A third possibility is that a small amount of Fe(II) exists in all recently prepared ferritin samples and is responsible for the observed ·OH radical. Since the amount of hydroxyl radical generated in H-chain ferritin is very limited, we did not pursue the mechanism of its formation any further.

Hydroxyl radical was also detected in HuLF (Figure 6, spectrum a) in accord with the reported production of H_2O_2

in this protein (*4*) and its inability to attenuate Fenton chemistry at low iron loading (Figure 3, curves d). The failure to show ·OH production in HuLF in a recent paper (*24*) is perhaps due to the lower protein concentration (0.22 μM) employed and to the use of a different spin-trapping reagent (DMPO). Interestingly, no hydroxyl radical is detected upon high Fe(II) loadings [>350 Fe(II)/HuLF] (Figure 6, spectra c and d), implying a gradual changeover to a mineral surface mechanism where O_2 is completely reduced to H_2O. HuLF is different from HuHF in that a "young Fe(III) core" in HuLF does not react with H_2O_2 at 350 Fe(III)/HuLF or higher to produce hydroxyl radical (Figure 6, spectra c and d), consistent with the cores of HuLF having greater crystallinity and stability than those of HuHF (*41*).

The reported cleavage of DNA from the longer term exposure to HuHF observed in in vitro experiments (*22*) could arise from ·OH produced from the putative reaction of H_2O_2 with the Fe(III) of the core as elaborated here. Alternatively, it has been noted that the presence of dithiothreitol (DTT) in ferritin solutions enhances DNA nicking (*22*). This reagent will reduce Fe(III) in the core of ferritin to Fe(II) and thus facilitate Fenton chemistry. The observed lag time required for the onset of DNA damage is probably due to the reduction and mobilization of iron from the protein (*22*), a process that would be promoted by DTT.

In closing, the spin-trapping data have established that HuHF attenuates hydroxyl radical formation from the Fenton reaction and that this property of the protein is likely the molecular basis for its protective effect on cells under oxidative stress. An intact ferroxidase site is required for this detoxification function. The small amount of hydroxyl radical formed during the oxidative deposition of iron in ferritin with either O_2 or H_2O_2 as oxidants appears to stem from the reaction of H_2O_2 with the Fe(III) core by an unspecified mechanism rather than from the Fenton reaction directly.

ACKNOWLEDGMENT

The authors thank Dr. Fadi Bou-Abdallah for helpful discussions and for obtaining the data in Figure 2 and Dr. Georgia Papaefthymiou for measuring the Mössbauer spectra.

REFERENCES

1. Harrison, P. M., and Arosio, P. (1996) Ferritins: Molecular properties, iron storage function and cellular regulation, *Biochim. Biophys. Acta 1275*, 161−203.
2. Chasteen, N. D., and Harrison, P. M. (1999) Mineralization in ferritin: An efficient means of iron storage, *J. Struct. Biol. 126*, 182−194.
3. Zamocky, M., and Koller (1999) Understanding the structure and function of catalases: clues from molecular evolution and *in vitro* mutagenesis, *Prog. Biophys. Mol. Biol. 72*, 19−66.
4. Zhao, G., Bou-Abdallah, F., Arosio, P., Levi, S., Janus-Chandler, C., and Chasteen, N. D. (2003) Multiple pathways for mineral core formation in mammalian apoferritin. The role of hydrogen peroxide, *Biochemistry 42*, 3142−3150.
5. Crichton, R. R., Herbas, A., Chavez-Alba, O., and Roland, F. (1996) Identification of catalytic residues involved in iron uptake by L-chain ferritins, *J. Biol. Inorg. Chem. 1*, 567−574.
6. Bou-Abdallah, F., Papaefthymiou, G., Scheswohl, D., S., Stanga, S., Arosio, P., and Chasteen, N. D. (2002) μ-1,2-peroxobridged di-iron(III) dimer formation in human H-chain ferritin, *Biochem. J. 364*, 57−63.
7. Treffry, A., Zhao, Z., Quail, M. A., Guest, J. R., and Harrison, P. M. (1995) Iron(II) oxidation by H chain ferritin: Evidence from site-directed mutagenesis that a transient blue species is formed at the dinuclear iron center, *Biochemistry 34*, 15204−15213.
8. Zhao, Z., Treffry, A., Quail, M. A., Guest, J. R., and Harrison, P. M. (1997) The early intermediate is not an iron tyrosinate, *J. Chem. Soc., Dalton Trans*., 3977−3978.
9. Pereira, A. S., Small, W., Krebs, C., Tavares, P., Edmondson, D. E., Theil, E. C., and Huynh, B. H. (1998) Direct spectroscopic and kinetic evidence for the involvement of a peroxodiferric intermediate during the ferroxidase reaction in fast ferritin mineralization, *Biochemistry 37*, 9871−9876.
10. Waldo, G. S., and Theil, E. C. (1993) Formation of iron(III)-tyrosinate is the fastest reaction observed in ferritin, *Biochemistry 32*, 13262−13269.
11. Zhao, G., Bou-Abdallah, F., Yang, X., Arosio, P., and Chasteen, N. D. (2001) Is hydrogen peroxide produced during iron(II) oxidation in mammalian apoferritins?, *Biochemistry 40*, 10832−10838.
12. Xu, B., and Chasteen, N. D. (1991) Iron oxidation chemistry in ferritin; increasing Fe/O_2 stoichiometry during core formation, *J. Biol. Chem. 266*, 19965−19970.
13. Jameson, G. N. L., Jin, W., Krebs, C., Perreira, A. S., Tavares, P., Liu, X., Theil, E. C., and Huynh, B. H. (2002) Stoichiometric production of hydrogen peroxide and parallel formation of ferric multimers through decay of the diferric-peroxo complex, the first detectable intermediate in ferritin mineralization, *Biochemistry 41*, 13435−13443.
14. Bou-Abdallah, F., Zhao, G., Mayne, H. R., Arosio, P., and Chasteen, N. D. (2005) Origin of the unusual kinetics of iron deposition in human H-chain ferritin, *J. Am. Chem. Soc. 127*, 3885−3893.
15. Yang, X., Chen-Barrett, Y., Arosio, P., and Chasteen, N. D. (1998) Reaction paths of iron oxidation and hydrolysis in horse spleen and recombinant human ferritins, *Biochemistry 37*, 9743−9750.
16. Bou-Abdallah, F., Lewin, A. C., Le Brun, N. E., Moore, G. R., and Chasteen, N. D. (2002) Iron detoxification properties of *Escherichia coli* bacterioferritin. Attenuation of oxyradical chemistry, *J. Biol. Chem. 277*, 37064−37069.
17. Lowery, T. J., Bunker, J., Zhang, B., Costen, R., and Watt, G. D. (2004) Kinetic studies of iron deposition in horse spleen ferritin using H_2O_2 and O_2 as oxidants, *Biophys. Chem. 111*, 173−181.
18. Bunker, J., Lowry, T., Davis, G., Zhang, B., Brosnahan, D., Lindsay, S., Costen, R., Choi, S., Arosio, P., and Watt, G. D. (2005) Kinetic studies of iron deposition catalyzed by recombinant human liver heavy, and light ferritins and *Azotobacter vinelandii* bacterioferritin using O_2 and H_2O_2 as oxidants, *Biophys. Chem. 114*, 235−244.
19. Cozzi, A., Corsi, B., Levi, S., Santambrogio, P., Albertini, A., and Arosio, P. (2000) Overexpression of wild type and mutated human ferritin H-chain in HeLa cells: *in vivo* role of ferritin ferroxidase activity, *J. Biol. Chem. 275*, 25122−25129.
20. Epsztejn, S., Glickstein, H., Picard, V., Slotki, I. N., Breuer, W., Beaumont, C., and Cabantchik, Z. I. (1999) H-ferritin subunit overexpression in erythroid cells reduces the oxidative stress response and induces multidrug resistance properties, *Blood 94*, 3593−3603.
21. Thompson, K. J., Fried, M. G., Ye, Z., Boyer, P., and Connor, J. R. (2002) Regulation, mechanisms and proposed function of ferritin translocation to cell nuclei, *J. Cell Sci. 115*, 2165−2177.
22. Surguladze, N., Thompson, K. M., Beard, J. L., Connor, J. R., and Fried, M. G. (2004) Interactions and reactions of ferritin with DNA, *J. Biol. Chem. 279*, 14694−14702.
23. Grady, J. K., Chen, Y., Chasteen, N. D., and Harris, D. (1989) Hydroxyl radical production during oxidative deposition of iron in ferritin, *J. Biol. Chem. 264*, 20224−20229.
24. Van Eden, M. E., and Aust, S. D. (2001) The consequences of hydroxyl radical formation on the stoichiometry and kinetics of ferrous iron oxidation by human apoferritin, *Free Radical Biol. Med. 31*, 1007−1017.
25. Treffry, A., Harrison, P. M., Luzzago, A., and Cesareni, G. (1989) Recombinant H-chain ferritins: effects of changes in the 3-fold channels, *FEBS Lett. 247*, 268−272.
26. Levi, S., Santambrogio, P., Cozzi, A., Rovida, E., Corsi, B., Tamborini, E., Spada, S., Albertini, A., and Arosio, P. (1994) The role of the L-chain in ferritin iron incorporation. Studies of homo and heteropolymers, *J. Mol. Biol. 238*, 649−654.
27. Treffry, A., Hirzmann, J., Yewdall, S. J., and Harrison, P. M. (1992) Mechanism of catalysis of Fe(II) oxidation by ferritin H-chains, *FEBS Lett. 302*, 108−112.

28. Bauminger, E. R., Harrison, P. M., Hechel, D., Nowik, I., and Treffry, A. (1991) Mössbauer spectroscopic investigation of structure−function relations in ferritins, *Biochim. Biophys. Acta 1118*, 48−58.
29. Zhao, G., Ceci, P., Ilari, A., Giangiacomo, L., Laue, T. M., Chiancone, E., and Chasteen, N. D. (2002) Iron and hydrogen peroxide detoxification properties of DNA-binding protein from starved cells: a ferritin-like DNA-binding protein of *Escherichia coli*, *J. Biol. Chem. 277*, 27689−27696.
30. Su, M., Cavallo, S., Stefanini, S., Chiancone, E., and Chasteen, N. D. (2005) The so-called *Listeria innocua* ferritin is a Dps protein. Iron incorporation, detoxification, and DNA protection properties, *Biochemistry 44*, 5572−5578.
31. Bou-Abdallah, F., Arosio, P., Santambrogio, P., Yang, X., Janus-Chandler, C., and Chasteen, N. D. (2002) Ferrous ion binding to recombinant human H-chain ferritin. An isothermal titration calorimetry study, *Biochemistry 41*, 11184−11191.
32. Wiedenheft, B., Mosolf, J., Willits, D., Yeager, M., Dryden, K. A., Young, M., and Douglas, T. (2005) An archaeal antioxidant: Characterization of a Dps-like protein from *Sulfolobus solfataricus*, *Proc. Natl. Acad. Sci. U.S.A. 102*, 10551−10556.
33. Gutteridge, J. M. C., Nagy, I., Maidt, L., and Floyd, R. A. (1990) ADP-iron as a Fenton reactant: radical reactions detected by spin trapping, hydrogen abstraction, and aromatic hydroxylation, *Arch. Biochem. Biophys. 277*, 422−428.
34. Perez-Benito, J. F. (2004) Iron(III)-hydrogen peroxide reaction: Kinetic evidence of a hydroxyl-mediated chain mechanism, *J. Phys. Chem. A 108*, 4853−4858.
35. Aruoma, O. I., Halliwell, B., Gajewski, E. and Dizdaroglu, M. (1989) Damage to the bases in DNA induced by hydrogen peroxide and ferric ion chelates, *J. Biol. Chem. 264*, 20509−20512.
36. Gutteridge, J. M. C., Maidt, L., and Poyer, L. (1990) Superoxide dismutase and Fenton chemistry. Reaction of ferric-EDTA complex and ferric-bipyridyl complex with hydrogen peroxide without the apparent formation of iron(II), *Biochem. J. 269*, 169−174.
37. Bou-Abdallah, F., Santambrogio, P., Levi, S., Arosio, P., and Chasteen, N. D. (2005) Unique iron binding and oxidation properties of human mitochondrial ferritin: A comparative analysis with human H-chain ferritin, *J. Mol. Biol. 347*, 543−554.
38. Bou-Abdallah, F., Adinolfi, S., Pastore, A., Laue, T. M., and Chasteen, N. D. (2004) Iron binding and oxidation properties of bacterial frataxin CyaY of *Escherichia coli*, *J. Mol. Biol. 341*, 605−615.
39. Ghio, A. J., Taylor, D. E., Stonehuerner, J. G., Piantadosi, C. A., and Crumbliss, A. L. (1998) The release of iron from different asbestos structures by hydrogen peroxide with concomitant O_2 generation, *BioMetals 11*, 41−47.
40. Bolann, B. J., and Ulvik, R (1990) On the limited ability of superoxide to release iron from ferritin, *Eur. J. Biochem. 193*, 899−904.
41. Wade, V. J., Levi, S., Arosio, P., Treffry, A., Harrison, P. M., and Mann, S. (1991) Influence of site-directed modifications on the formation of iron cores in ferritin, *J. Mol. Biol. 221*, 1443−1452.

BI052443R